Erzincan Üniversitesi
Fen Bilimleri Enstitüsü Dergisi
2020, 13(3), 1025-1041
ISSN: 1307-9085, e-ISSN: 2149-4584
Araştırma Makalesi

Erzincan University
Journal of Science and Technology
2020, 13(3), 1025-1041
DOI: 10.18185/erzifbed.707837
Research Article

Effects of Magnet Type and Thickness on Outer Rotor Brushless Direct Current Motor Design

Alper Sefa ÇAĞIŞLAR[1], Sedat İN[2], Hasan TİRYAKİ[3*]

[1, 2, 3] Istanbul University - Cerrahpaşa, Electrical and Electronics Engineering Department, 34320, Istanbul, Turkey

Geliş / Received: 23/03/2020, Kabul / Accepted: 07/10/2020

Abstract

While electric vehicles are taking their place as today's transportation vehicles, big R&D investments are being made by automobile manufacturers. Outer and inner rotor motors are used for electric vehicles. Considering the fact that the transmission organs make the structure more complex, outer rotor motors come into prominence in applications requiring small power. This study includes the design of outer rotor brushless direct current motor for electric vehicle prototypes. In addition, the effects of magnet type and magnet thickness on the design were analyzed in detail. The effects of magnet type and magnet thickness selected in the design of outer brushless direct current motor can be observed from the results, especially effecting power and torque parameters.

Keywords: Outer Brushless Direct Current Motor, Design, Magnet Type, Magnet Thickness, Efficiency, Power, Torque

Bir Elektrikli Araç Prototipi İçin Gerekli Motor Gücü Hesaplanarak Tasarlanan Dış Rotorlu Fırçasız Doğru Akım Motoruna Mıknatıs Tipinin ve Kalınlığının Etkileri

Öz

Elektrikli araçlar günümüzün ulaşım araçları olarak yerini alırken otomobil üreticileri tarafından bu konuda büyük Ar-Ge yatırımları yapılmaktadır. Bu konuda popülerleşen elektrikli araçlar için dışsal ve içsel rotorlu motorlar kullanılmaktadır. Aktarım organlarının yapıyı daha karmaşıklaştırdığı göz önünde bulundurulduğunda dışsal rotorlu motorlar küçük güç gerektiren uygulamalarda verimlilikleri ile ön plana çıkmaktadır. Bu çalışma prototip elektrikli araçlar için dış rotorlu fırçasız doğru akım motoru tasarımını içermektedir. Ayrıca yapılan analizler ile mıknatıs tipinin ve mıknatıs kalınlığının tasarıma etkileri detaylı olarak incelenmiştir. Elde edilen sonuçlar; kullanılan mıknatıs tipinin ve kalınlığının fırçasız doğru akım motorunun tasarımında dikkat edilmesi gereken verim, güç ve tork parametrelerine etkilerini net olarak gözler önüne sermektedir.

Anahtar Kelimeler: Fırçasız Doğru Akım Motoru, Tasarım, Mıknatıs Tipi, Mıknatıs Kalınlığı, Verim, Güç, Tork

1. Introduction

The transportation sector continues to evolve in different ways with today's technology. High-efficiency electric vehicles, which are increasing in use and which do not harm the environment, are being preferred by the technology developing day by day. Electric cars, motorcycles, skateboards and many other technological vehicles are attracting worldwide attention and are moving rapidly towards becoming the indispensable

technology of the future. The motor to be selected under all these conditions is really important.

Direct current motors are widely used in industrial applications. Limited use of brushed models in some areas has enabled Brushless DC motors to stand out. Need for continuous maintenance of brushed-type motors provides disadvantage in variable conditions and in the areas of continuous use. For this reason, brushless DC motors have a wide range of applications. Brushless DC motors come to the forefront with performance values such as high efficiency and high torque.

Direct current motors are motors in which the magnetic field is produced by means of magnets. The magnet can be an electromagnet or permanent magnet. When a permanent magnet is used to create a magnetic field in a direct current motor, the motor is called a permanent magnet direct current motor or a permanent magnet brushless direct current (BLDC) motor (Hanselman, 2003).

Brushless direct current motor is in fact configured as a rotating magnet through a series of coil-carrying conductors. Current in the conductors and the magnets that are arranged in order for the torque to be in one direction need to be positively positioned as the rotation takes place. Direct current is carried out by the pole switching commutator and brushes in commutator motor. Since the commutator is fixed to the rotor, switching events are automatically synchronized with the alternating polarity of the magnetic field through which the conductors pass. Polarity of the brushless DC motor is carried out by the power transistors which must be switched in synchronous with the rotor position. The commutation process is similar in two machines, and the resulting performance equations and speed / torque concepts are almost identical.

Brushless DC motors with outer rotor type are used for applications requiring high torque and inertia. This type of motors are used in many areas such as vehicle wiper motor, automatic windows, robotic, generator, electric vehicles, unmanned aerial vehicles, white goods sector (Yedemale, 2003). Although there are various disadvantages such as motor protection and resistance to shocks in outer rotor applications, it is preferable that applications do not need any transfer components because they provide direct drive of the moment. In addition, the motor drives used for brushless DC motors have a more complex structure than other motors. Due to the high torque values of outer rotor brushless direct current motors, they are used in electric vehicles in particular (Pahlavani, et al., 2017).

In the electric vehicle prototypes, direct drive brushless direct current motors are preferred due to their higher efficiency. However, in order to keep efficiency in the maximum range, the motors must be designed and manufactured in accordance with the vehicle and its features. It is very important to determine the correct magnet type and thickness, as well as many parameters during the design phase.

In this study, an outer rotor brushless DC motor is designed for an electric vehicle prototype. While designing, the effects of the magnet type and magnet thickness used in the desired speed ranges on the efficiency, power and torque parameters to be considered in the design of the brushless DC motor are examined comparatively and the

optimal magnet type and magnet thickness has been determined for design.

2. Material and Methods

Since the effects of the effects of magnet type and thickness to be used in this study will be examined in the motor design, a detailed study has been done in this section. The other parameters are described below.

2.1 Determination of power and porque parameters for motor design

The motor to be designed will be the BLDC motor with outer rotor. In the case of outer rotor motor applications, a design can be realized without the need for any transferring systems and ignoring the losses of this transfer organ. The greatest advantage of these motors is the direct transfer of torque (Tiryaki et al., 2017). Figure 1 shows the forces affecting the vehicle.

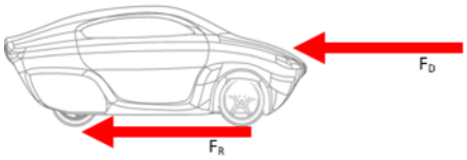

Figure 1: The forces affecting the vehicle.

Design requirements for the outer BLDC can be defined using following equations:

$$F_D = \frac{1}{2}.\rho.V^2.A.C_D \quad (1)$$

Wind Friction Force (WFF) formed by air on an object is shown in equation 1. F_D air friction force, ρ air density, V object velocity, A is the object's cross-sectional surface area and C_D is the object's aerodynamic friction coefficient.

Another force to be calculated for the vehicle is the Rolling Resistance Force (RRF).

$$F_R = f_s.m.g \quad (2)$$

F_R is defined as friction force. fs is the coefficient of friction of the tire used and g is the force of gravity.

The forces of F_D and F_R, which constitute the fundamental forces of the vehicle, are involved in the determination of torque and power requirements as motor parameters. Considering Figure 1, the necessary moment calculations related to these forces are calculated by considering the force and force arm rule.

$$\tau_D = F_D.r_D \quad (3)$$

The amount of torque required to resist wind is given in Equation 3. τ_D represents the amount of torque required and r_D represents the distance from the center of the surface density center of the vehicle to the center of the wheel.

$$\tau_R = F_R.r_R \quad (4)$$

The required torque calculation against rolling resistance is given in Equation 4. τ_R represents the amount of torque required and the distance between the r_R ground and the center of the wheel.

$$\tau_{motor} = \tau_D + \tau_R \quad (5)$$

When Equation 3 and Equation 4 are combined, the amount of torque that the motor must produce at a certain speed, as in Equation 5, arises.

$$w_{rpm} = \frac{V.1000}{60.2\pi.R} \quad (6)$$

Equation 6 represents the speed of the w_{rpm} wheel in rpm. V is the radius of the wheel in km / h as speed and R meter.

$$w_{motor} = \frac{w_{rpm}.2\pi}{60} \quad (7)$$

In equation 7 w_{motor} as an angular velocity its in radial/sec.

$$P_{motor} = \tau_{motor}.w_{motor} \quad (8)$$

In the light of the necessary calculations, the equation of power in Equation 8, which we can describe in general, emerges. P_{motor} refers to the rated power of the motor. The nominal power of the motor is calculated and two factors occur in the design phase that affect many parameters of the motor (Tiryaki et al., 2017).

The parameters of the vehicle to be applied should be determined within the framework of high engineering and analysis. The vehicle planned to be implemented is the AZAK prototype electric racing vehicle produced by the MilAT 1453 Electromobile R&D Society and the most efficient vehicle record in 2017 ever made in the Efficiency Challenge organized by the TUBİTAK.

The information about the AZAK vehicle, which has been produced by the Department Istanbul University - Cerrahpaşa, is shown in Table 1.

Table 1: Parameters of the vehicle AZAK.

VEHICLE INFORMATION	VALUES
Reference velocity	*V= 56 km/h=15.51 m/sn*
Weight of the vehicle	*m=215 kg*
Radius of the tire used	*R=0.279 meters*
Friction Coef. Of the tire used	*C=0.009*
Front surface of the vehicle subject to friction	*A=1.18 m^2*
Friction coefficient of the vehicle (The result of aerodynamic analysis)	*C_D=0.07*
Air Density	*ρ=1.225 kg/m^3*
The distance from the center of the vertical section of the vehicle to the wheel hub	*r_D=0.32 meters*

Depending on motor usage and load, varying power and torque values must be determined (Pahlavani, et al., 2017). Calculations according to the weight of the vehicle to be used and the speed required to determine the nominal values are described above.

The nominal speed of the motor to be used for the electric vehicle varies depending on the wheel diameter and the rated speed. 56 km/hour value is calculated for the vehicle planned to be done and the number of rotations were determined.

The calculations were made assuming that the forces to be defeated were WFF and RRF.

Table 2: Calculated design values.

Calculated Values	Results
Wind Friction Force	*F_D =12.17 N*
Rolling Resistance Force	*F_R =18.98 N*
Acceleration Force	*Fm=94 N*
Total Needed Torque	*τ_{motor}=9.2 Nm*
Revolution of Tires	*w_{rpm} = 532.42 d/d*
Angular Speed	*w_{motor}=55.75 rad/sn*
Nominal Power	*P_{motor}=512.9 W*

As shown in Table 2, the torque required to move the BLDC motor at 56 km / h was 9.2 Nm and the rated power was 512.9 W.

The torque required to reach a speed of 56 km / h in 30 seconds is set at 28.93 Nm and the maximum power required is approximately 1.5 kW (Cagislar, 2018).

2.2 Determination of battery voltage

One of the features that should be determined during the design phase is the determination of the slot-pole combination of the motor. This parameter fundamentally affects the stator and rotor design of the motor.

Increasing the number of poles means increasing the number of magnets, which increases the torque generated. When the studies corresponding to the number of slots corresponding to the number of poles are examined, the winding factor should be considered (Jafarboland and Sargazi, 2018).

The winding factor is calculated using electromotive force phasors. For this purpose, the number of poles and slots of the motor with winding factor must be determined (Luo et al., 2018). Battery features are given in Table 3.

Table 3: Battery features.

Features	Values
Operating voltage	48 V
Parallel Number	12
Serial Number	12
Total Power	1632 Watt

2.3 Determination of slot-pole combination

One of the features that should be determined during the design phase is the determination of the slot-pole combination of the motor. This parameter fundamentally affects the stator and rotor design of the motor.

When the studies corresponding to the number of slots corresponding to the number of poles are examined, the winding factor should be considered (Jafarboland and Sargazi, 2018).

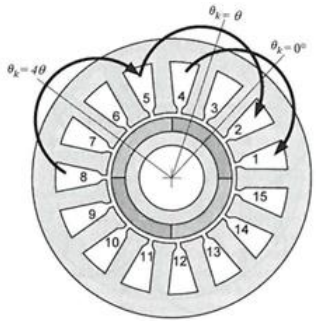

Figure 2: Motor with four poles and fifteen slots (Hanselman, 2003).

The image of the relative angular deviation of the coils of the motor is shown in Figure 2. The expression of the angle is as in Equation 9.

$$\theta_k = (k-1)\frac{N_m}{N_s}180^{\circ}E \qquad (9)$$

θ_k, refers to the relative angular deviation of coil k. N_m is shown as the number of poles and N_s is the number of slots.

$$K_{wn} = \frac{1}{N_{cph}}\sum_{k=1}^{N_{cph}} e^{-jn\theta_k} \qquad (10)$$

Equation 10 is the equation of the winding factor. Here the K_{wn} represents winding factor, N_{cph} is the number of slots per phase. n is the harmonic index, and θ is the relative angular deviation of the coil k (Hanselman, 2003).

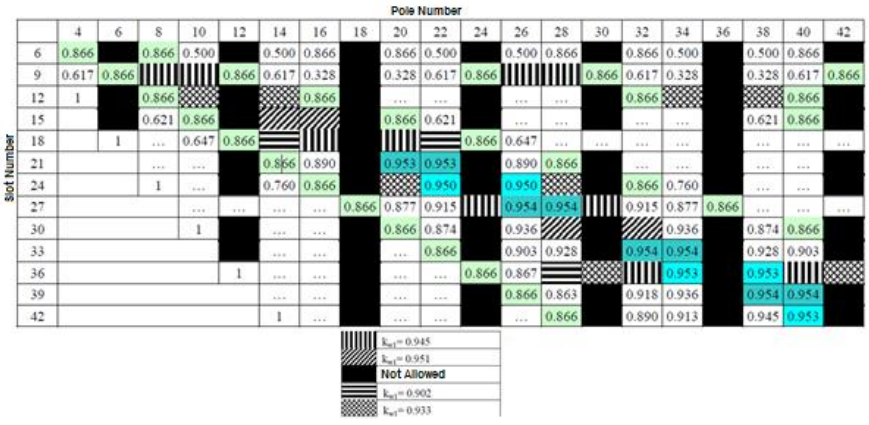

Figure 3: Winding factor values corresponding to the slot-pole combination.

The winding factor responses corresponding to the slot-pole combinations are shown in Figure 3. k_{w1} refers to the first harmonic winding factor. The winding factor refers to the ability of the electrical power applied to the motor to be converted to torque (Libert and Soulard, 2004).

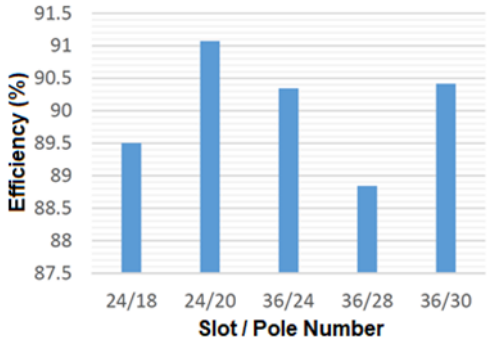

Figure 4: The effect of slot-pole combination on efficiency.

The values shown in Figure 4 affects the determination of the output power, operating temperature, stator slot occupancy rate and air gap constant determined at the beginning of the design (Cabuk et al., 2016).

Table 4: Comparison of the slot/pole combination to efficiency.

Slot-Pole Combination	Winding Factor	Effciency (%)
24/20	0.933	91.1
36/24	0.866	90.3
36/28	0.902	88.9
36/30	0.933	90.4

As shown in Table 4, the winding factor positively affects the efficiency. The motor is designed in accordance with the usage area and the most effective value is chosen by considering the location or cost factors of the motor.

As described above, a slot-pole combination should be chosen to keep the winding factor high (Ma et al., 2018). In terms of cost, it is aimed to provide the need of application with high power density by making a selection that keeps the number of magnets higher, since there is no obstacle in the prototype based studies.

The slot-pole combination was determined as 36/32 the most suitable for the prototype determined. The slot-pole combination to be selected can vary and the selected value affects the design in different ways.

2.4 Determination of motor dimensions and structural parameters

In terms of motor design, the location of the motor is the pioneer in determining many parameters such as stator and rotor dimensions of the motor, determination of slot-pole combination and magnet dimensions.

The dimensions to be chosen here are determined according to the space behind the wheel in electric vehicle prototype. These dimensions of the motor are composed of stator and rotor.

2.4.1 Stator parameters

The dimensions of the stator of the motor and the properties of the materials in the stator part are given in Table 5.

Table 5: Stator features.

Features	Values/Types
Outer Radius	240 mm
Inner Radius	180 mm
Width	30 mm
Sheet Type	Steel_1010
Stacking Factor	0.95
Tilt Width	0

The inclination width represents the slope of the stator slots. With this feature, different designs are provided. At the design stage, this value will be 0 and there will be no slope.

Figure 5 shows the laminated ferromagnetic material. The compression factor range, which is also found in the stator parameters, is typically chosen in the range of 0.8 to 0.99 (Hanselman, 2003).

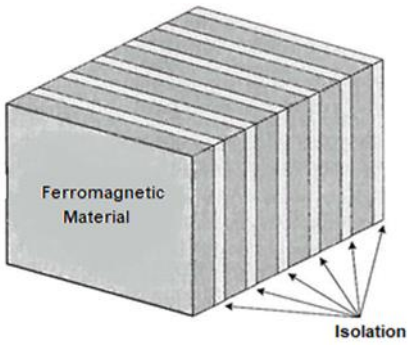

Figure 5: Laminated ferromagnetic material.

The parameters determined when we consider the motor's winding type are shown in Table 6.

Table 6: Winding parameters.

Features	Values/Types
Windings Number	12
Winding Layer	2
Connection Type	Half Coiled
Parallel Winding Nr.	1
Coil Range	1
Slot Occupancy Ratio	0.6

The number of parallel windings refers to the number of parallel wires to be used for the winding. The number of conductors in the slot corresponds to twice the total winding for double layer winding. This is because there are two coil sides per slot.

The value referred to as coil spacing indicates that the next conductor wire of a coil will come out of the slot. The slot occupancy ratio gives the ratio of the volume of conductive and insulating materials in a slot to the volume of the entire slot.

2.4.2 Rotor parameters

The dimensions of the rotor of the motor that is designed as an outer rotor and the information contained in the rotor part are given in Table 7.

Table 7: Rotor features.

Features	Values/Types
Outer Radius	260 mm
Inner Radius	244 mm
Width	30 mm
Sheet Type	Steel_1010
Stacking Factor	1
Pole Frequency	0.96

The metal material used to reduce the effect of eddy currents is laminated as thin as possible and covered with insulating material. The flow permeability of the material is not lost here, but the eddy currents that will occur are reduced. The stacking factor refers to the loss of lamination resulting from the material when calculating the flux of the material. It is available from the manufacturer's catalogs. This factor in stator hair produced by lamination method is considered to be 1 for the rotor planned to be made from one piece (Cagislar, 2018).

Pole frequency often encountered in polar design is the value indicating how often the magnets to be placed on the rotor are placed in the rotor frame.

3. Numerical Results and Discussion

Finite element method is an emerging technique to solve the problems expressed by partial differential equations. This method which takes place in the field of engineering in the solution of these problems day by day is biomechanical, heat transfer, stress, electromagnetic, aerodynamic and so on are used in many areas.

The analysis of the parameters with the parameters will be carried out by ANSYS Maxwell Electromagnetics Suite 16.0.0 (Maxwell, 2015). The results of this method will be examined.

In the analyzes to be performed, the speed will be targeted and the design analysis for the determined speed value will be examined.

The most effective factor on the basis of design is magnet type and thickness properties will be examined and the differences in motor design against these features will be examined. In order to make an objective evaluation, the same values were used for all parameters except magnet type and thickness in each simulation and especially the working voltage was kept at 48 V and the wire diameter was kept constant at 1.29 mm (Cagislar, 2018).

3.1 Effects of magnet type

The choice of magnet type is an important parameter in the motor design. Neodymium magnets are more widely used than other types of magnets due to their wider area of use and price performance characteristics (Mhango, 1989).

Some models of Neodymium magnets on analysis studies will be discussed (Shen et al., 2017), (Prosperi et al., 2018). The properties of some neodymium magnets are shown in Table 8.

Analysis studies were performed with 5 different magnet types shown in Table 8. The results of the selection of these magnet types in motor design are examined.

Table 8: Magnet types and features (Cagislar, 2018).

Type	Operating Temp.	Permanent Induction		Residual Magnetization Force		Maximum Energy Product
	T (°C)	Br(kGs)		Hcb	Hcj	$(BH)_{max}$
		Min	Max	kOe	kOe	MGOe
N35-M	100	11.8	12.5	11	14	37
N40-M	100	12.6	13.2	11.8	14	42
N45-M	100	13.2	13.8	12.2	14	46
N48-M	100	13.7	14.3	12.6	14	49
N50-M	100	14	14.6	12.8	12	51

Examining the table 8, with the increase of the model numbers of magnets, BH_{max} value also increases. The efficiency, power and torque values of the motor are calculated according to the speed parameter taken as reference.

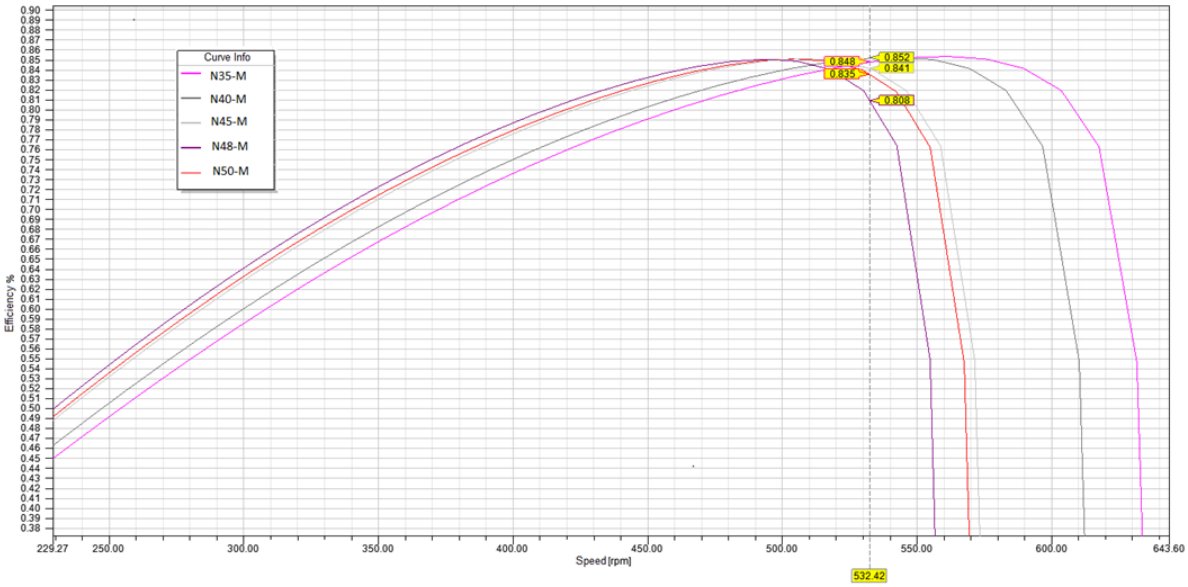

Figure 6: Effect of magnet type on efficiency-speed curve.

3.1.1 Effect of magnet type on efficiency

The addition of the features of magnets shown in Table 8 and along these information, efficiency-speed curve is given in Figure 6.

It is seen that the maximum speed value decreases when the efficiency graph which is produced by increasing the magnet power is examined in general. When the graph is examined according to the specified speed value, the values which are seen at 532.42 rpm are shown in Table 9.

Table 9: Efficiency values corresponding to magnet types.

Magnet Type	Efficiency Value (%)
N35-M	84.8
N40-M	85.2
N45-M	84.1
N48-M	83.5
N50-M	80.8

When Table 9 was examined, a difference of less than 1.5% was observed between the values of the other magnets except the N50-M magnet.

3.1.2 Effect of magnet type on power

The power-speed curve corresponding to 5 different magnet types is shown in Figure 7. Other parameters were kept constant while graphics were created. In Figure 7, when the power-speed curve is examined in general, it has been observed that when the magnet power is reduced, the curve increases and the maximum speed value increases and the maximum power value decreases.

Table 10 shows the power values corresponding to the magnet type specified for the reference speed value. Considering the power value indicated in the design phase, it is observed that N48-M and N45-M models are closer to this value.

Table 10: Power values corresponding to magnet types.

Magnet Type	Power Value
N35-M	1.16 kW
N40-M	0.98 kW
N45-M	0.59 kW
N48-M	0.54 kW
N50-M	0.39 kW

3.1.3 Effect of magnet type on torque

Figure 8 shows the torque-speed curve determined by 5 different magnet types. When this curve is examined in general, it is seen that the maximum speed increases when the magnet power is reduced.

Table 11 shows the torque values corresponding to the magnet type according to the reference speed value.

Table 11: Torque values corresponding to magnet types.

Magnet Type	Torque Value
N35-M	20.77 Nm
N40-M	17.59 Nm
N45-M	10.56 Nm
N48-M	9.64 Nm
N50-M	6.98 Nm

When Table 11 was examined, the torque is increased at this reference value by decreasing the magnet power at the speed taken as a reference.

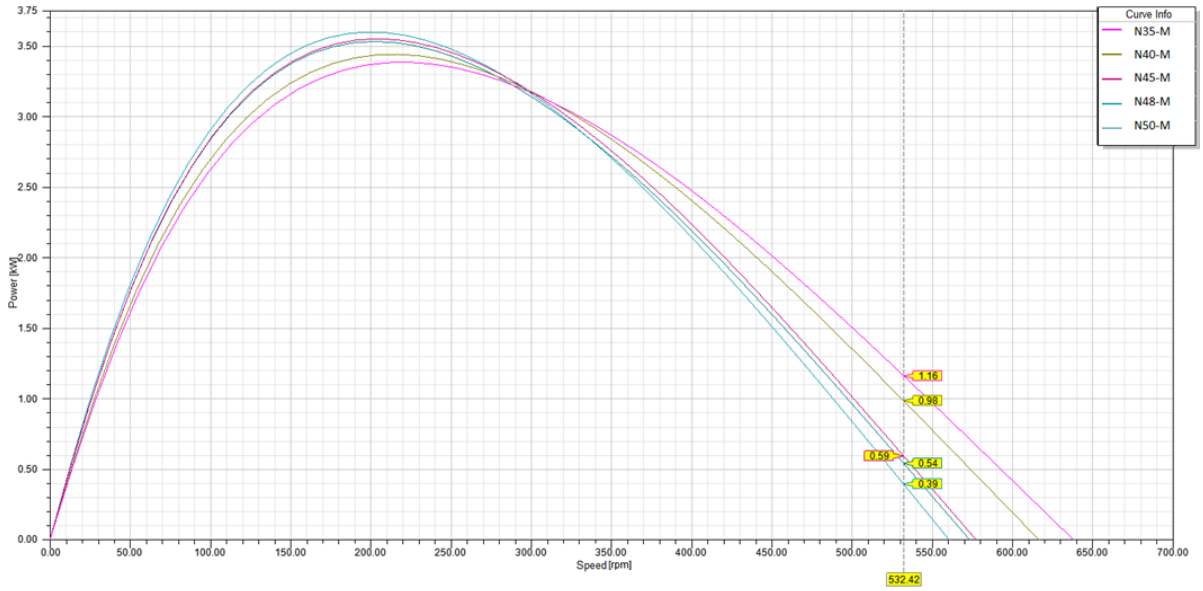

Figure 7: Effect of magnet type on power-speed curve.

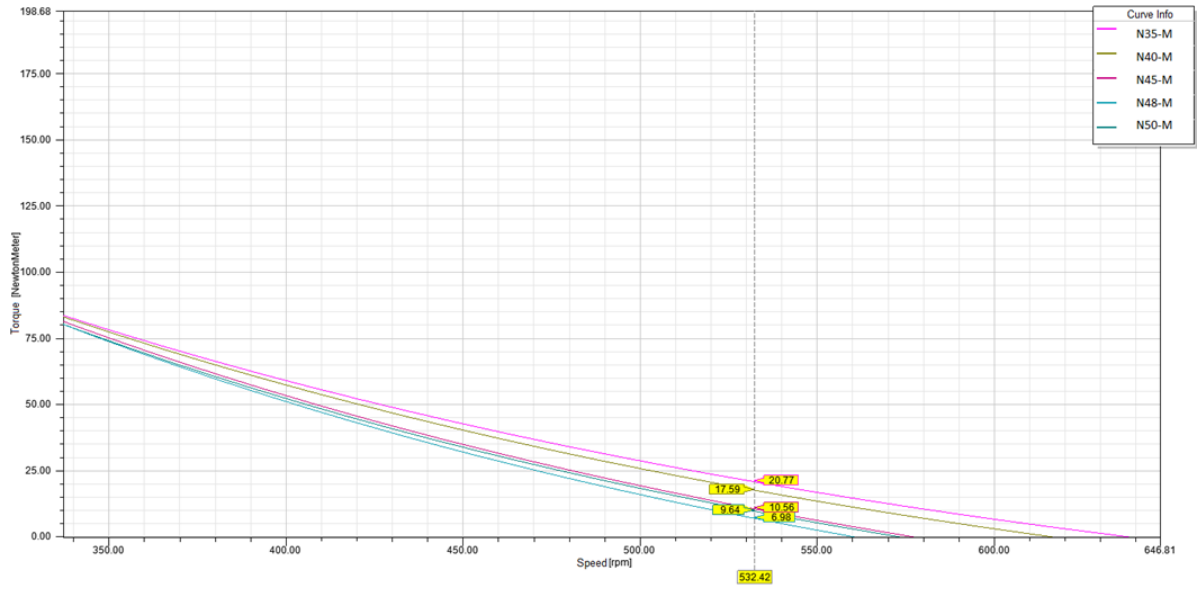

Figure 8: Effect of magnet type on torque-speed curve.

3.1.4 Magnetic and electrical effects of magnet type

As a result of the design difference made according to the magnet type, many parameters are affected in the analysis phase. Some of these parameters will be emphasized.

Depending on the number of windings and the magnet power density, the flux density formed by the magnetic field formed by these structures on the sheet should not exceed a certain value. This value should be taken into consideration considering the B-H curve of the sheet material used for the stator.

When the density of a magnetic flux above the BH curve is applied on the material, the material reaches saturation and this saturation adversely affects the design in terms of efficiency. In summary, the saturation area of the hysteresis curve of the selected material should be determined and revised studies should be performed considering these values as a result of the design (Ziegenbein, 2011).

The B-H curve of the Steel 1010 product used in the design phase is given in Figure 9 (Fezzani and Amor, 2013).

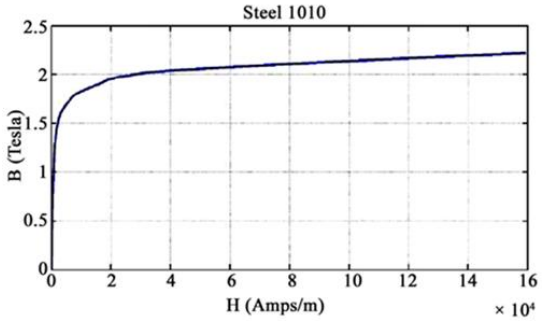

Figure 9: B-H graph of silicon steel sheet.

The space between the teeth and the rotor and the stator is called the air gap. The flux density in this area is considered as a research topic in itself. As a result of the studies carried out, the value of the flux density in this area, the value of an external magnetic field and the permanent point of the magnets as a magnetic field acts as a magnetic field (Kim et al., 2016). The flux density in the air gap causes an impact that causes vibrations and vibrations, which leads to vibrations called cogging and reduces motor performance (Oztura and Canbaz, 2003).

Figure 10 shows the magnetic flux densities of the motor generated according to the design parameters determined using the Ansys Maxwell 2D Design plug-in.

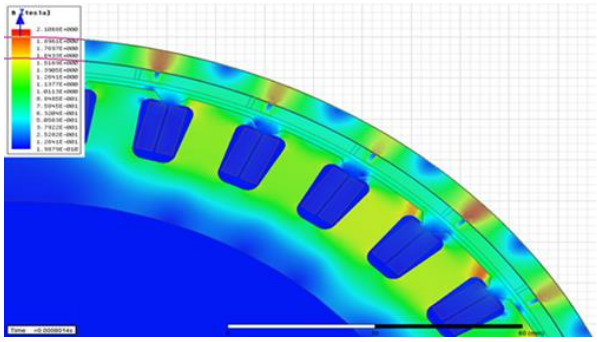

Figure 10: Display of magnetic flux densities with Ansys Maxwell 2D.

When considering the flux density on the stator, there should be stator teeth since the place to be observed is exposed to more flux density than the area per unit. The Ansys Maxwell 2D Design plug-in, which has been regionally inspected on the stator, provides clearer magnetic flux densities.

Table 12: Stator outer flux density, air gap flux density, armature current density and iron losses according to magnet type.

Magnet Type	Stator Outer Flux Density (T)	Air Gap Flux Density (T)	Armature Current Density (A/mm^2)	Iron Losses (W)
N35-M	1.43	0.59	5.09	44.26
N40-M	1.48	0.61	4.09	47.41
N45-M	1.58	0.65	2.10	54.07

N48-M	1.63	0.67	1.18	57.35
N50-M	1.69	0.69	0.87	62.27

When the stator thread flux density values are examined in Figure 10 and Table 12, this value is lower than 1.6 T for N45-M model neodymium magnet and it is the magnet with the lowest current luminaire density.

As a result, the N-45-M magnet type was found to be more suitable than the other magnet types because it provides espcesially power and torque values for the electric vehicle prototype studied.

3.2 Effects of magnet thickness

The effects of a magnet thickness determined in this section will be examined. N45-M neodymium magnet which is selected in the design stage and which is the most suitable magnet type mentioned above for this study will be studied and its effects on different thicknesses will be examined. The specified magnet thicknesses are shown in Table 13.

Table 13: Effects of magnet thicknesses to be studied.

Number	N45-M Magnet Thickness
1	2 mm
2	2.4 mm
3	2.8 mm
4	3.2 mm
5	3.6 mm

The point that should be considered when using the Ansys Maxwell program is that the maximum value of the selected magnet thickness should be the half that of the determined rotor outer diameter and the internal diameter difference. As shown in Table 7, the maximum diameter of the magnet that can be given is 8 mm, as indicated by the outer diameter 260 mm and the inner diameter 244. However, this value is an ideal value and it is not possible by giving this value because the rotor thickness is selected by the magnet completely. Depending on the determined magnet thickness values, the thickness of the rotor except the magnet is reduced.

For the 5 different magnet thicknesses according to the reference speed, power, efficiency and torque graphs plotted in the Ansys Maxwell Design (Maxwell, 2015) program.

3.2.1 Effect of magnet thickness on efficiency

Figure 11 shows the effects of the designs created according to the magnet thicknesses by combining the efficiency. When the shape is examined, it is seen that the yield peaks are at the same levels. It is observed that the maximum speed value increases with decreasing the magnet thickness.

The efficiency values of the magnets with the thickness specified in Table 14 are shown as the reference speed value of 532,42 rpm.

Table 14: Efficiency values corresponding to magnet thicknesses.

Magnet Thickness	Efficiency Value (%)
2 mm	83.9
2.4 mm	85.1
2.8 mm	84.1
3.2 mm	74.8
3.6 mm	-

When Table 14 is examined, a corresponding efficiency value of 532.42 rpm is not seen for the design created with a magnet of 3.6 mm thickness. This is due to the fact that the graph corresponding to the magnet having a thickness of 3.6 mm when viewed in Figure 11 is below this speed value and ends at a lower speed. 2 mm, 2.4 mm and 2.8 mm thickness magnets in the design of the

efficiency values are observed to create a difference of maximum 0.1% of each other.

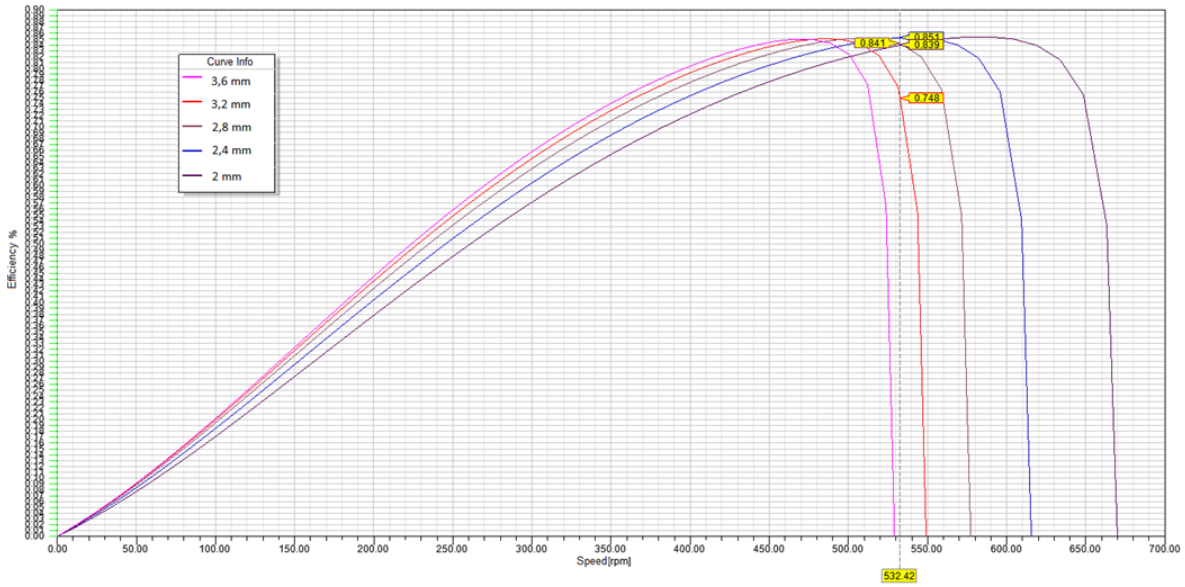

Figure 11: Effect of magnet thickness on efficiency-speed curve.

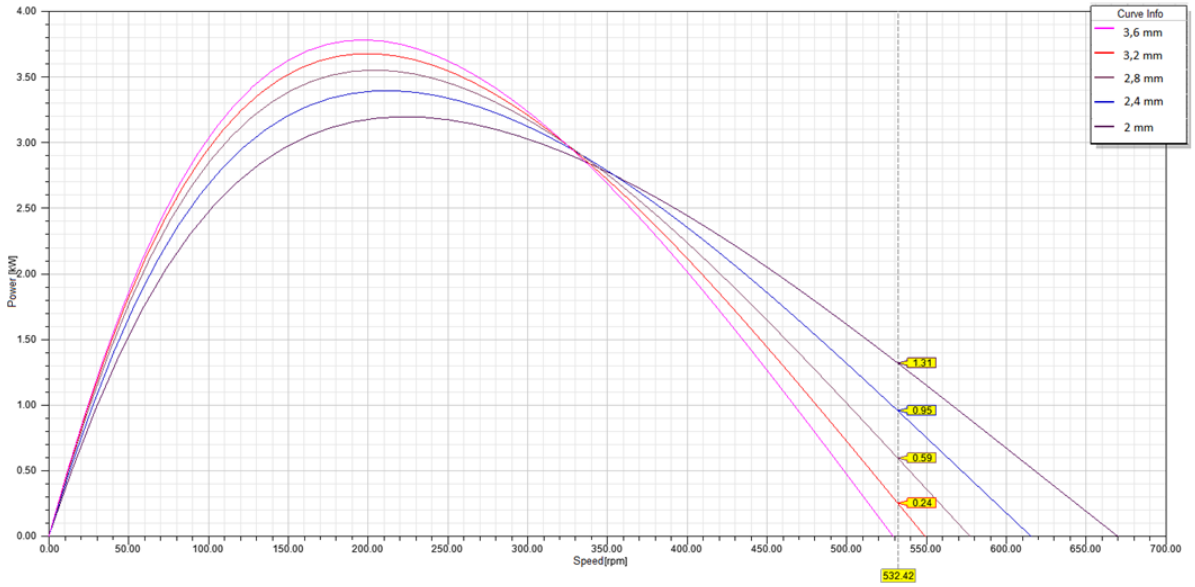

Figure 12: Effect of magnet thickness on power-speed curve.

3.2.2 Effect of magnet thickness on power

Figure 12 shows the power-velocity curves corresponding to 5 different magnet types. When these curves are examined, it can be clearly deduced that the magnet thickness is directly proportional to the maximum power. Maximum magnitude increases as the magnet thickness increases and maximum speed decreases.

Table 15 shows the power values corresponding to magnet thicknesses at a speed of 532.42 rpm. With a 3.6 mm thickness design, this speed value is not available in the power-speed curve. Considering the power value mentioned in the design phase, it is seen that the magnet

design of 2.8 mm thickness is the closest value when Table 15 is examined.

Table 15: Power values corresponding to magnet thicknesses.

Magnet Thickness	Power Value
2 mm	1.31 kW
2.4 mm	0.95 kW
2.8 mm	0.59 kW
3.2 mm	0.24 kW
3.6 mm	-

3.2.3 Effect of magnet thickness on torque

Figure 13 shows the torque-velocity curves corresponding to the magnet thicknesses. When these curves were examined, it was observed that the starting torque decreased with the decrease in the magnet thickness.

Table 16 shows the torque values corresponding to magnet thicknesses of 532.42 rpm.

Table 16: Torque values corresponding to magnet thicknesses.

Magnet Thickness	Torque Value
2 mm	2.57 Nm
2.4 mm	17.85 Nm
2.8 mm	10.56 Nm
3.2 mm	4.38 Nm
3.6 mm	-

In Table 2, the determined torque value for 532.42 rpm is shown as 9.2 Nm. When the values in Table 16 are considered, the torque value corresponding to the magnet model of 2.8 mm thickness is shown as 10.56 Nm. This value is seen as the closest value to the other values in the table.

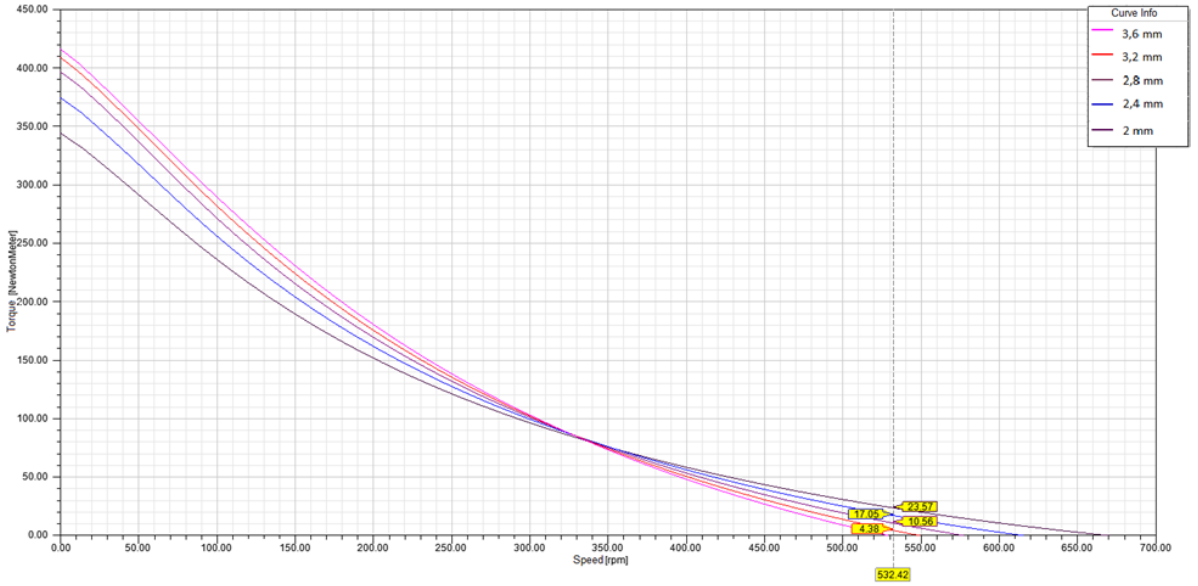

Figure 13: Effect of magnet thickness on torque-speed curve.

3.2.4 Magnetic and electrical effects of magnet thickness

It has been observed that the magnetization effect is decreased by decreasing the thickness when various studies are performed for the effects of changing the magnet thickness. In addition, it has been shown by several studies that it also reduces the cogging effect (Vidhya and Srinivas, 2017).

Table 17: Stator outer flux density, air gap flux density, magnet flux density and armature leak inductance according to magnet thickness

Magnet Thickness	Stator Outer Flux Density (T)	Air Gap Flux Density (T)	Magnet Flux Density (T)	Armature Leak Inductance (Henry)
2 mm	1.37	0.56	0.62	0.000383
2.4 mm	1.48	0.61	0.68	0.000374
2.8 mm	1.58	0.65	0.73	0.000368
3.2 mm	1.66	0.69	0.77	0.000362
3.6 mm	1.72	0.72	0.80	0.000357

When the values in Table 17 were examined, it was seen that the magnetic flux density on the stator increased with the increase in magnet thickness. This increases in proportion to the flux density applied by the magnet. Depending on the thickness of the magnet, the magnetic flux generated also increases. The magnetic flux formed by the magnet on the sheet is also indicated by the values determined in Table 17 where the flux is increasing due to its thickness (Tiryaki et al., 2016).

The luminaire leakage inductance symbolizes the inductance of the coil, which symbolizes the magnetic flux lines that do not result in the desired magnetic direction. This inductance value of the magnetic flux which has no effect on the magnetization of the coil within the coil and magnet relationship is determined in the environment. Figure 14 shows the magnetic flux lines of the motor designed with the Ansys Maxwell 2D insert (Stazak, 2013).

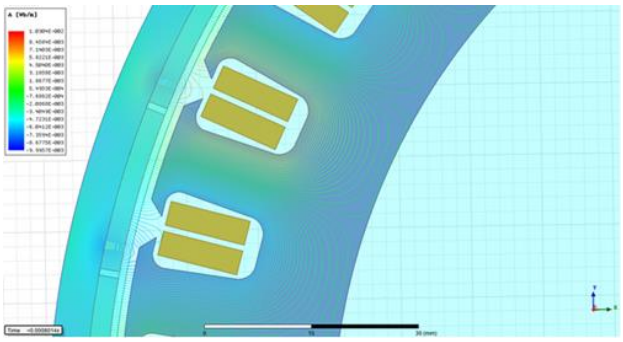

Figure 14: Display of magnetic flux lines with Ansys Maxwell 2D.

As a result, the 2.8 mm magnet thickness was found to be more suitable than the other magnet thickness because it provides espcesially power and torque values for the electric vehicle prototype studied.

4. Conclusion

While electric vehicles are taking their place as today's transportation vehicles, big R&D investments are made by automobile manufacturers. Outer and inner rotor motors are used for electric vehicles. Considering the fact that the transmission systems make the structure more complex, outer rotor motors come into prominence in applications requiring small power.

In the electric vehicle prototypes, direct drive brushless direct current motors are preferred due to their higher efficiency. However, in order to keep efficiency in the maximum range, the motors must be designed and manufactured in accordance with the vehicle and its features. It is very important to determine the correct magnet type and thickness, as well as many parameters during the design phase. It is very important to determine all motor parameters specific to the vehicle to which the motor will be applied during the design phase.

In this study, the design parameters determined according to the physical, electrical and magnetic needs of the motor, which constitute the design input parameters, were obtained. These parameters include a number of substances, such as values and physical measurements, determined by the aerodynamic analysis of the vehicle to be used. In order to calculate the input parameters of the motor which is designed in the light of these values, necessary information has been realized with the help of many articles and academic studies.

The study includes the design of the BLDC motor for the electric vehicle prototypes. In addition, the effects of magnet type and magnet thickness on the design were analyzed in detail. The relationship between other magnet types and magnet sizes has been examined considering all possibilities. As a result of these investigations, it was concluded that N45-M neodymium magnet which is the most suitable magnet type and the most suitable thickness for this type of magnet is 2.8 mm for the motor design.

In addition to the analytical solutions made with ANSYS Maxwell RMxprt module, the proposed motor will be verified by using the transient analysis with 2D/3D FEM Model before production. In the near future, it is planned to start the production from the motor design and to make analyzes based on experimental results and to contribute to the literature.

5. Acknowledgements

This study was funded by the Scientific Research Projects Coordination Unit of Istanbul University - Cerrahpasa. Project numbers: 52033

6. References

Cabuk AS, Saglam S, Tosun G, Ustun O. (2016) “Investigation of different slot-pole combinations of an ın-wheel BLDC motor for light electric vehicle propulsion.” *International Conference on ELECO’16*, Bursa, Turkey.

Cagislar AS. (2018) “Brushless Direct Current Motor Design for Electric Vehicles.” MSc Thesis, *Institute of Graduate Studies In Sciences*, Istanbul University, Istanbul, Turkey. (In Turkish)

Fezzani WE, Amor AB. (2013) “Finite element methods applied to the tubular linear stepping motor.” *Journal of Electromagnetic Analysis and Applications*, 5(5), 219-222.

Hanselman D. (2003) “Brushless Permanent Magnet Motor Design.” 9nd ed. Lebanon, *Magna Physics Publishing*.

Jafarboland M, Sargazi MM. (2018) “Analytical modelling of the effect of pole offset on the output parameters of BLDC motor”. *IET Electric Power Applications*, 12(5), 666-676.

Kim YS, Kim JY, Kang DW, Lee J. (2016) “Reliability analysis of permanent magnet and air-gap flux density of spoke-type ıpmsm for driving cooling fans”. *Indian Journal of Science and Technology*, 9(14), 1-6.

Libert F, Soulard J. (2004) “Investigation on pole-slot combinations for permanent-magnet machines with concentrated windings”. *International Conference on Electric Machines (ICEM’’04)*, Cracow, Poland.

Luo Y, Zhu Y, Yu Y, Zhang L. (2018) “Inductance and force calculations of circular coils with parallel axes shielded by a cuboid

of high permeability". *IET Electric Power Applications*, 12(5), 717-727.

Ma C, Li Q, Lu H, Liu Y, Gao H. (2018) "Analytical model for armature reaction of outer rotor brushless permanent magnet DC motor". *IET Electric Power Applications*, 12(5), 651-657.

Maxwell, (2015) "ANSYS Maxwell Electromagnetics Suite 16.0.0", Reference Manual.

Mhango LMC. (1989) "Benefits of Nd-Fe-B magnet in brushless DC motor design for aircraft applications". *Fourth International Conference on Electrical Machines and Drives*, London, England, 13-15 September.

Oztura H, Canbaz H. (2003) "Analysis of reduction of torque in no-load conditions in permanent magnet variable air range motors". *10th Electical – Electronics – Computer Engineering Congress*, Istanbul, Turkey, 18-21. (In Turkish)

Pahlavani MRA, Ayat YS, Vahedi A. (2017) "Minimisation of torque ripple in slotless axial flux BLDC motors in terms of design considerations". *IET Electric Power Applications*, 11(6), 1124–1130.

Prosperi D, Bevan AI, Ugalde G, Tudor CO, Furlan G, Dove SK, Lucia P, Zakotnik M. (2018) "Performance comparison of motors fitted with magnet-tomagnet recycled or conventionally manufactured sintered NdFeB". *Journal of Magnetism and Magnetic Materials*, 460(2018), 448-453.

Shen S, Tsoi M, Prosperi D, Tudor CO, Dove SK, Bevan AI, Furlan G, Zakotnik M. (2017) "A comparative study of magnetoresistance and magnetic structure in recycled vs. virgin NdFeB-type sintered magnets". *Journal of Magnetism and Magnetic Materials*, 422(2017), 158-162.

Staszak J. (2013) "Determination of slot leakage inductance for three-phase induction motor winding using an analytical method". *Archives of Electrical Engineering*, 62(4), 569-591.

Tiryaki H, Akgündoğdu A, Erdoğan G, Karadeniz O, Şahin U, Yılmaz MY, Durak Y, Kocaarslan I. (2017) "Implementation of an electromobile for efficiency challenge". *World Electro Mobility Conference (WELMO'17)*, Izmir, Turkey. (In Turkish)

Tiryaki H, Cagislar AS, Akgundogdu A, Kocaarslan I. (2016) "Commutable magnetic field on brushless direct current motor for electrical vehicle". *International Journal of Engineering Research and Development*, 8(2), 37-45. (In Turkish)

Vidhya B, Srinivas KN. (2017) "Effect of stator permanent magnet thickness and rotor geometry modifications on the minimization of cogging torque of a flux reversal machine". *Turkish Journal of Electrical Engineering & Computer Sciences*, 25(2017), 4907-4922.

Yedemale P. (2003) "Brushless DC (BLDC) Motor Fundamentals". *Microchip Technology Inc.*, USA, App. Note: DS00885A.

Ziegenbein J. (2011) "Magnetic Clamping Structures for The Consolidation of Composite Laminates". PhD Thesis (PhD), *Georgia Institute of Technology*, North Ave NW/Atlanta, USA.